Melting curve of two-dimensional Yukawa systems predicted by isomorph theory

Nichen Yu,[1] Dong Huang,[1,*] and Yan Feng[1,2,†]

[1]*Institute of Plasma Physics and Technology, Jiangsu Key Laboratory of Frontier Material Physics and Devices, School of Physical Science and Technology, Soochow University, Suzhou 215006, China*

[2]*National Laboratory of Solid State Microstructures, Nanjing University, Nanjing 210093, China*

(Received 2 May 2024; accepted 4 June 2024; published 20 June 2024)

The analytical expression for the conditions of the solid-fluid phase transition, i.e., the melting curve, for two-dimensional (2D) Yukawa systems is derived theoretically from the isomorph theory. To demonstrate that the isomorph theory is applicable to 2D Yukawa systems, molecular dynamical simulations are performed under various conditions. Based on the isomorph theory, the analytical isomorphic curves of 2D Yukawa systems are derived using the local effective power-law exponent of the Yukawa potential. From the obtained analytical isomorphic curves, the melting curve of 2D Yukawa systems is directly determined using only two known melting points. The determined melting curve of 2D Yukawa systems well agrees with the previous obtained melting results using completely different approaches.

DOI: 10.1103/PhysRevE.109.065212

I. INTRODUCTION

The isomorph theory [1–6] refers to the theory of the hidden scale invariance [6], which is widely investigated in various liquids and solids [7–13]. Specifically, the isomorph theory suggests that various liquids and solids exhibit quasi-invariant curves, i.e., isomorphic curves or isomorphs, along which some properly reduced structural and dynamical quantities are approximately invariant in the thermodynamic phase diagram [5,6]. Usually, the isomorph theory applies to the Roskilde-simple (R) systems [12], where there are strong correlations between the virial and potential energy equilibrium fluctuations [6]. Previous investigations suggest that most van der Waals bonded, metallic, as well as weakly ionic or dipolar systems exhibit the isomorphic curves, while most directional bonded systems, such as water, do not [1,6–8]. Furthermore, it is found that the model systems with the interactions of the inverse power law [8,10], the Lennard–Jones [1–3,5], the Buckingham [8], etc., also exhibit the isomorphic curves.

Dusty (complex) plasma [14–21] consists of many micron-size dust particles in the plasma environment, which exhibit collective behaviors. Under the typical laboratory conditions, these dust particles are highly charged to $\sim -10^4$ elementary charges, so that they interact with each other through the Yukawa repulsion [22]

$$\phi_{\mathrm{Y}}(r) = \frac{Q^2}{4\pi\epsilon_0 r}\exp\left(-\frac{r}{\lambda_D}\right), \tag{1}$$

where λ_D is the Debye screening length and Q is the charge on each dust particle. The potential energy between neighboring dust particles is significantly higher than their kinetic energy, i.e., these dust particles are strongly coupled, exhibiting the solidlike or liquidlike properties [23–45]. Due to the gravity effect, these dust particles are able to self-organize into a single layer [15], i.e., a two-dimensional (2D) suspension, in the plasma sheath [24–33,46]. The individual particle motion can be directly captured by video imaging and then analyzed by particle tracking [47], so that dusty plasma provides an excellent model to study various fundamental physical procedures, including melting [44,48–51], at the individual particle kinetic level [52].

To quantitatively investigate the properties of dust plasmas under various conditions, the Yukawa systems are usually used in simulations and theories [53–55]. Dusty plasmas and Yukawa systems are traditionally characterized by the coupling parameter $\Gamma = Q^2/4\pi\epsilon_0 a k_B T$ and the screening parameter $\kappa = a/\lambda_D$ [17,19,20,23]. Here, k_B is the Boltzmann constant, T is the kinetic temperature of particles, and a is the Wigner-Seitz radius, which is $a = (1/\pi n)^{1/2}$ [23] for 2D systems, where n is the particle number density.

The conditions of the solid-fluid phase transition, i.e., the melting curve for 2D dusty plasmas, have been systematically investigated in both simulations [56,57] and theories [51,55]. Based on Lindemann's melting criterion [55,58] and the characteristic oscillation frequency [59], the melting curve of 2D Yukawa systems is derived theoretically in Ref. [55]. Using computer simulations of 2D Yukawa systems under vast ranges of conditions [56,57], the melting curves of 2D Yukawa systems are obtained from the empirical formula fitting based on the static structural diagnostics. Recently, the reduced transverse sound speed in 2D Yukawa systems is found to be isomorph invariant [60], which can also be used as a criterion to predict the melting curve [51]. However, it remains unknown whether it is possible to analytically derive the melting curve of 2D Yukawa systems entirely on the basis of the isomorph theory [6], as we study in this paper. In addition, due to the pure repulsion between dust particles, dusty plasmas exhibit the typical properties of supercritical

*Contact author: huangdong@suda.edu.cn
†Contact author: fengyan@suda.edu.cn

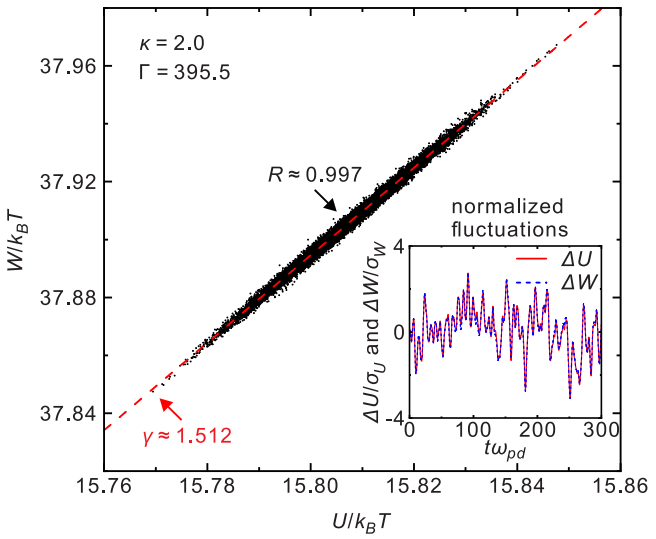

FIG. 1. Scattering plot of the calculated instantaneous virial W and potential energy U for the 2D Yukawa system of $\kappa = 2$ and $\Gamma = 395.5$. The dashed line corresponds to the standard linear-regression slope of $\gamma \approx 1.512$. The calculated R value 0.997 is larger than 0.9, clearly indicating that this 2D Yukawa system is a typical R system. The inset shows the time series of the normalized fluctuations of virial ΔW and potential energy ΔU, clearly indicating that W and U are strongly correlated. Note that σ_W and σ_U correspond to the standard deviation of W and U, respectively.

fluids at higher temperatures and their supercritical transition points between the liquidlike and gaslike states are studied in Ref. [61].

The rest of the paper is organized as follows. In Sec. II, we briefly review the isomorph theory and then introduce our simulation methods. In Sec. III, we demonstrate that the isomorph theory is still applicable to 2D Yukawa systems using our simulation data. We also report our derived analytical isomorphic curves of 2D Yukawa systems, which are later used to determine the melting curve of 2D Yukawa systems. In Sec. IV, a brief summary of our findings is provided.

II. ISOMORPH THEORY REVIEW

The isomorph theory [1–5] originates from the discovery of a number of model liquids exhibiting strong correlations between the virial and potential energy equilibrium fluctuations [1,7]. These strong correlations, as in Fig. 1(a) of Ref. [7], are presented through the time series of the normalized fluctuations of virial and potential energy which are nearly synchronized. These correlations are usually quantified using the Pearson correlation coefficient R [2] defined as

$$R = \frac{\langle \Delta W \Delta U \rangle}{\sqrt{\langle (\Delta W)^2 \rangle \langle (\Delta U)^2 \rangle}}, \tag{2}$$

where Δ denotes the deviation from the corresponding average. Traditionally [2], a system can be considered as a Roskilde-simple (R) system when its Pearson correlation coefficient R is larger than 0.9. Another important property of these strong correlations is that the instantaneous virial and potential energy nearly exhibit the linear relation, as shown in Fig. 1(b) of Ref. [7]. Therefore, as an important characteristic quantity, the density-scaling exponent γ [1,5] is defined using standard linear-regression slope as

$$\gamma = \frac{\langle \Delta W \Delta U \rangle}{\langle (\Delta U)^2 \rangle}. \tag{3}$$

For R systems, the existence of the hidden scale invariance, i.e., the isomorphic curves, has been demonstrated in their thermodynamic phase diagram [3,5,6]. From the definition [6], the hidden scale invariance refers to the reduced physical quantities, i.e., those normalized by macroscopic thermodynamic quantities, for example, $n^{-1/d}$, $m^{1/2}(k_BT)^{-1/2}n^{-1/d}$, and k_BT as the units of the length, time, and energy, respectively [62,63], where d is the dimensionality of the studied system. While expressed in the reduced units, some physical quantities are approximately invariant along the isomorphic curves, which are called isomorph invariants [5,6]. A number of physical quantities in the reduced units are found to be isomorph invariant, such as the excess entropy, the viscosity, the transverse sound speed, the radial distribution function, and the mean-squared displacement [6,60,64].

Using the thermodynamic theories, the previously discovered isomorphic properties can be derived analytically [5,9]. Based on the Maxwell relations and the canonical ensemble theory, previous investigation [5] shows that Eq. (3) can be rewritten as

$$\gamma = \left(\frac{\partial \ln T}{\partial \ln n} \right)_{S_{ex}}, \tag{4}$$

where S_{ex} is the excess entropy defined following the deviation from the entropy of the ideal gas. As a thermodynamic quantity, Eq. (4) indicates the change rate of temperature with number density of constant excess entropy, i.e., the change rate along an isomorphic curve. In addition, for R systems, when S_{ex} and n are chosen as state parameters [9], the temperature k_BT is described as

$$k_BT = f(s_{ex})h(n). \tag{5}$$

Here, $s_{ex} = S_{ex}/k_BN$, which is the reduced excess entropy [63], while $f(s_{ex})$ and $h(n)$ are the thermodynamic functions corresponding to the contribution of the reduced excess entropy s_{ex} and number density n to the temperature k_BT, respectively. Since the reduced excess entropy s_{ex} is an isomorph invariant, from Eq. (5), it is reasonable to describe an isomorphic curve [9] as

$$\frac{h(n)}{k_BT} = \mathcal{K}, \tag{6}$$

where $\mathcal{K}$ is an arbitrary constant. Taking Eq. (6) into Eq. (4), the density-scaling exponent γ [9] can be expressed as

$$\gamma(n) = \frac{\mathrm{d} \ln h(n)}{\mathrm{d} \ln n}. \tag{7}$$

Equation (7) implies that, along an isomorphic curve, the density-scaling exponent γ is only dependent on the number density n.

From the statistical mechanics [6,65], the isomorph theory can be conveniently described using

$$U(\mathbf{R}) \cong h(n)\tilde{\Phi}(n^{1/2}\mathbf{R}) + g(n). \tag{8}$$

Here, $\tilde{\Phi}$ is the potential energy normalized by $h(n)$ under the reference density, $g(n)$ is the function of number density, and $\mathbf{R}$ is the collective $2N$-dimensional position vector defined by $\mathbf{R} = (\mathbf{r}_1, \ldots, \mathbf{r}_N)$ for 2D systems. Physically, Eq. (8) indicates that the potential-energy surface $U(\mathbf{R})$ approximately undergoes a linear affine transformation when the number density n changes [6]. Based on Eq. (8), nearly all important properties of R systems can be analytically derived, as presented in details in Refs. [6,64,65].

Aside from the results above, the inverse power law (IPL) potential $\phi_{\rm I}(r) \propto r^{-\alpha}$ is usually used to study the isomorphic properties in the previous investigations [1,2]. As derived in [2,3,6], the system with the IPL particle interaction exhibits the perfect correlation with $R = 1$ and the corresponding isomorphic curves can be directly derived analytically. Furthermore, various thermodynamic quantities [3,66] are always able to be described exactly using simple analytical expressions based on the excess Helmholtz free energy [3]. As a result, it is convenient to use the IPL potential to fit other interparticle interactions, so that the isomorphic properties of various R systems can be described easily using analytical expressions. As demonstrated in Refs. [2,10], a better choice to fit other interaction potentials is the extended inverse power law (eIPL) potential [2], where one linear term and one constant term are added to the IPL potential. The traditionally used eIPL potential is defined as

$$\phi_{\rm e}(r) = A(r/a)^{-\alpha} + Br/a + C, \tag{9}$$

where α is the power-law exponent and the coefficients A, B, and C are all constants to be determined.

The previous investigations [1–12,64,65,67–69] have demonstrated that the isomorph theory is applicable to various 3D systems with different interactions. Recently, the approximate isomorphic curves $\Gamma/\Gamma_{\rm m} = $ const are discovered in 2D Yukawa fluids based on the structural and dynamical diagnostics [60], where $\Gamma_{\rm m}$ is the coupling parameter at the solid-fluid phase transition point for 2D Yukawa systems in Refs. [55–57]. However, it remains unknown whether the isomorph theory still works in 2D dusty plasmas or 2D Yukawa systems. To systematically investigate the applications of the isomorph theory to 2D dusty plasma or 2D Yukawa systems, we perform equilibrium molecular dynamical (MD) simulations of 2D Yukawa systems under various conditions. Our specified κ values vary between 0.5 and 5.0, while the relative coupling parameter $\Gamma/\Gamma_{\rm m}$ values are chosen between 0.1 and 2.0. Other simulation details are the same as Refs. [60,70,71].

III. RESULTS

A. Isomorph theory demonstration in 2D Yukawa systems

From the analyzed results of our simulation data, we find that the virial W and potential energy U for 2D Yukawa systems are strongly correlated. For the studied conditions of $\kappa = 2.0$ and $\Gamma = 395.5$ in Fig. 1, obviously, the obtained instantaneous virial W and potential energy U results nearly exhibit a linear relation, with the standard linear-regression slope of $\gamma \approx 1.512$, which is also termed as the density-scaling exponent [1,5]. To visualize these strong correlations more clearly, we also plot the time series of the normalized fluctuations of virial ΔW and potential energy ΔU in the inset of Fig. 1. Using Eq. (2), the calculated R value is ≈0.997, significantly larger than 0.9, further indicating that this 2D Yukawa system is one typical R system. In fact, besides the conditions of Fig. 1, we confirm that, for 2D Yukawa systems under all simulated conditions studied here, the obtained R values are always >0.9, i.e., W and U are always strongly correlated.

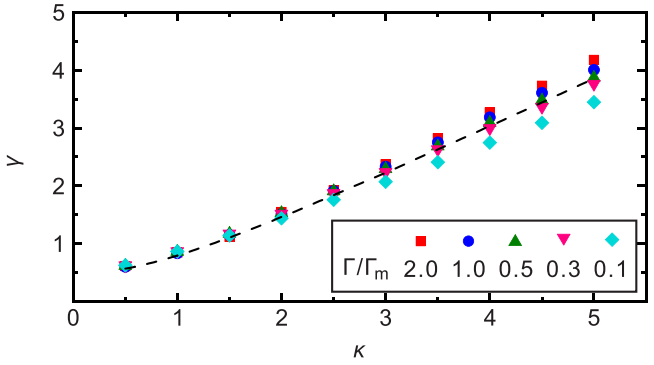

FIG. 2. Calculated density-scaling exponent γ from Eq. (3) for 2D Yukawa systems under different conditions. Clearly, the obtained γ values nearly exhibit a monotonic universal scaling with κ, no matter how $\Gamma/\Gamma_{\rm m}$ varies. The dashed curve corresponds to the analytical γ of Eq. (16) with determined $\Lambda \approx 0.957$ for $\Gamma/\Gamma_{\rm m} = 1.0$. Note that, for $\Gamma/\Gamma_{\rm m} = 0.1$, the obtained γ values at larger κ values are slightly lower than those for higher $\Gamma/\Gamma_{\rm m}$ values.

From Fig. 2, we find that the obtained density-scaling exponent γ exhibits a monotonic universal scaling for 2D Yukawa systems under different conditions. As shown in Fig. 2, the γ value is almost independent of the relative coupling parameter $\Gamma/\Gamma_{\rm m}$, almost only varying with the κ value, or equivalently the number density n as in [5,60,64], when assuming the Debye screening length λ_D is an environment length scale. In addition, from Fig. 2, we also find that the γ value gradually deviates from the universal scaling as the relative coupling parameter $\Gamma/\Gamma_{\rm m}$ decreases to the lower value of 0.1. From our understanding, this may be attributed to the effect of the higher temperature. As mentioned in [60], the isomorphic curve of $\Gamma/\Gamma_{\rm m} = $ const is only an approximate expression, which is more accurate at lower temperatures. For the much higher temperatures such as $\Gamma/\Gamma_{\rm m} = 0.1$, their accuracy diminishes slightly. As also found in [6,60], the isomorph theory gradually becomes unreliable when the system gradually approaches the gaslike state [61]. The temperature of our studied condition of $\Gamma/\Gamma_{\rm m} = 0.1$ is about half of the transition point between the liquidlike and gaslike states [61], probably slightly higher for the isomorph theory.

In Fig. 3, we present the sketch of using the eIPL potential to fit the Yukawa potential under the conditions of $\kappa = 2$ and $\Gamma = 395.5$. From Ref. [2], the fitting region should contain nearly all information within the first peak of the radial distribution function $g(r)$. To include nearly all information of the first peak of $g(r)$, we choose the lower and upper limits as the first nonzero value of $g(r)$ and the first minimum of $g(r)$, respectively, as presented in Fig. 3(b). For our studied 2D Yukawa systems under $\kappa = 2$ and $\Gamma = 395.5$, our choice of the fitting region is just $1.37 \lesssim r/a \lesssim 2.60$ from Fig. 3(b). Note that the fitting regions are slightly different for different

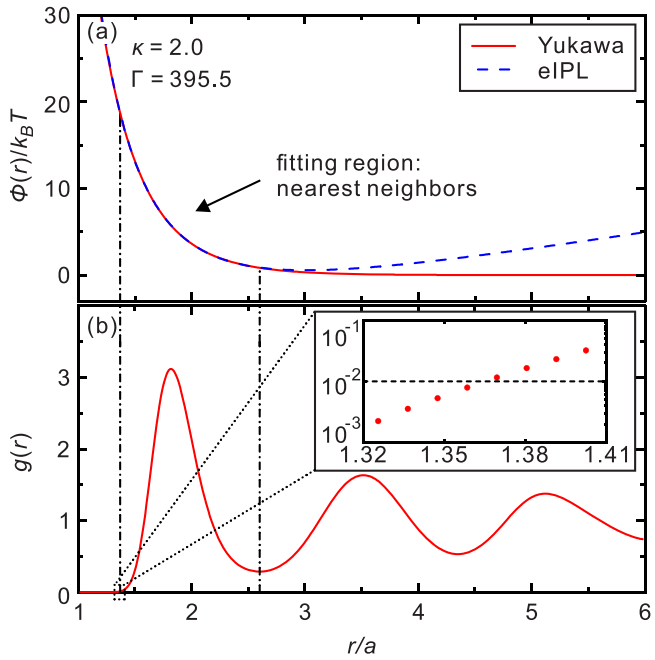

FIG. 3. (a) Sketch of using the eIPL potential to fit the Yukawa potential and (b) the corresponding radial distribution function $g(r)$ of the 2D Yukawa system under $\kappa = 2.0$ and $\Gamma = 395.5$. As in Ref. [2], the fitting region contains nearly all information within the first peak of $g(r)$. For the information of the first peak of $g(r)$, we choose the region of $1.37 \lesssim r/a \lesssim 2.60$, just corresponding to the locations of the first nonzero value of $g(r)$ and the first minimum of $g(r)$, respectively, as two dot-dashed lines shown. Note that the criterion to identify the first nonzero value of $g(r)$ corresponds to the first data point of $g(r) \geqslant 10^{-2}$, as shown in the magnified version in the inset of (b).

conditions, since the locations of the first nonzero value of $g(r)$ and the first minimum for $g(r)$ shift slightly as the system conditions vary.

Next, we are able to describe some physical properties of 2D Yukawa systems directly using the eIPL potential within our fitting region. As shown in Fig. 3, for the region of $r \gtrsim 3a$, clearly, the eIPL potential is dominated by the linear term Br/a, leading to the eIPL potential deviating from the Yukawa potential. However, from Refs. [6,8,64], the contribution of the linear term Br/a to the fluctuations of virial W or potential energy U is trivial. For the linear term Br/a, when a particle moves, the distance between some nearest neighbors decreases, while it may increase for others, leading to the approximately unchanged summation finally [2,6,64]. It is also demonstrated in Ref. [8] that the structure and dynamics of R liquids are given completely by the interactions within the first coordination shell. Therefore, we are able to describe the Yukawa systems approximately using the eIPL potential even for the range of $r \gtrsim 3a$.

To further illustrate the accuracy of using the eIPL potential to fit the Yukawa potential, we calculate the density-scaling exponent γ of 2D Yukawa systems based on the eIPL potential. Here, we follow Ref. [2] to obtain the density-scaling exponent results for 2D Yukawa systems using

$$\gamma = \alpha/2, \tag{10}$$

TABLE I. Comparison of the density-scaling exponent γ results obtained from two different methods for $\Gamma/\Gamma_m = 1.0$. Here, the γ_1 values are calculated from the simulated data using Eq. (3), while the γ_2 values are obtained from the exponent of Eq. (9), i.e., using the eIPL potential to fit the Yukawa potential as described in Fig. 3. Clearly, the obtained values of γ_1 and γ_2 are nearly identical, indicating the reliability of using the eIPL potential in 2D Yukawa systems.

κ	γ_1	γ_2
0.5	0.600	0.588
1.0	0.833	0.853
1.5	1.150	1.198
2.0	1.512	1.583
2.5	1.913	1.985
3.0	2.333	2.383
3.5	2.754	2.795
4.0	3.185	3.193
4.5	3.610	3.612
5.0	4.008	3.997

where the obtained γ results are labeled as γ_2 in Table I. For comparison, we also calculate the γ results directly from the simulation data using Eq. (3) directly, which are labeled as γ_1 in Table I. Obviously, the obtained γ_1 and γ_2 results are nearly identical, with the corresponding relative error less than 4.7% for $\Gamma/\Gamma_m = 1.0$. Note that Eq. (10) holds strictly for the IPL potential, while approximately for the eIPL potential [2,3].

B. Analytical isomorphic curves derivation

To obtain the analytical isomorphic curves of 2D Yukawa systems, a reasonable approach is to find the analytical expression of the thermodynamic function $h(n)$ in Eq. (6). Since the expression of density-scaling exponent γ in Eq. (7) contains $h(n)$, we are able to derive $h(n)$ directly through $\gamma(n)$. Comparing the different methods described above in obtaining the γ value, we believe that the choice of Eq. (10) is the most convenient.

To obtain the expression of γ from Eq. (10), we follow Refs. [2,64,69] to determine the power-law exponent of the Yukawa system α_Y from the so-called local effective power-law exponent [2,64,69] defined as

$$\alpha^{(p)}(r) = -r\frac{\phi^{(p+1)}(r)}{\phi^{(p)}(r)} - p. \tag{11}$$

Here, $\phi^{(p)}(r)$ denotes the pth-order derivative of the interparticle interaction $\phi(r)$, which is the Yukawa repulsion for our current investigation. However, by directly substituting the Yukawa repulsion into Eq. (11), the expression of $\alpha^{(p)}(r)$ is always complicated, no matter how the p value varies. To determine the most suitable choice of p with the convenient analytical derivation in the expression of $\alpha^{(p)}(r)$, we replace the Yukawa potential using the eIPL potential in Eq. (11), as demonstrated in Fig. 3 and Table I. We find that, for the eIPL potential of Eq. (9), the right-hand side (RHS) of Eq. (11) always equals the constant of α when $p \geqslant 2$. To satisfy the requirement of $p \geqslant 2$, in the latter derivation, we follow Refs. [2,64,69] to choose $p = 2$, corresponding the

lowest derivative of Eq. (11) with the simplest mathematical derivations.

Next, we substitute $p = 2$ and the Yukawa potential of Eq. (1) into the RHS of Eq. (11), while using the α value of the eIPL potential on the LHS of Eq. (11), leading to a new equation of the distance r. In fact, the RHS of this new equation is just a function of r. Since the structure and dynamics of R liquids are given completely by the interactions within the first coordination shell [8], the solution of r to satisfy the new equation described above should be close to the nearest-neighbor distance labeled as $r = \Lambda n^{-1/2}$, as demonstrated in [64,69], where Λ is the reduced nearest-neighbor distance, an unknown value close to unity. As a result, we are able to obtain the density-scaling exponent γ for 2D Yukawa systems using $\alpha^{(2)}(r)$ as

$$\gamma(n) = \left.\frac{\alpha^{(2)}(r)}{2}\right|_{r=\Lambda n^{-1/2}}. \tag{12}$$

Here, we follow [2,64,69] to choose $p = 2$ in our derivations, because the previous investigations [2,64,69] have demonstrated that the information within the first peak of $g(r)$ can be well described using $\alpha^{(2)}(r)$ when $r = \Lambda n^{-1/2}$. Note, in principle, one may also choose $p > 2$ in derivations, although the corresponding mathematical procedures would be much more complicated.

Since the $\gamma(n)$'s analytical expression of Eq. (12) for Yukawa systems is obtained, we are able to derive the analytical expression of $h(n)$ from Eq. (7) directly. To solve this differential equation more simply, we follow Refs. [64,69] to rewrite Eq. (12) as $\gamma(n) = d\ \ln[r^2\phi^{(2)}(r)/2]/d\ \ln r$ when $r = \Lambda n^{-1/2}$. Combining this new expression of $\gamma(n)$ with Eq. (7), we obtain

$$h(n) = \mathcal{A} r^2 \phi^{(2)}(r)|_{r=\Lambda n^{-1/2}}, \tag{13}$$

where $\mathcal{A}$ is an arbitrary constant. Substituting the Yukawa interaction of Eq. (1) and the relation of $n^{-1/2} = \sqrt{\pi}a$ into Eq. (13), we obtain

$$h(\kappa) = \frac{\mathcal{A}}{a}\left(\frac{2}{\sqrt{\pi}\Lambda} + 2\kappa + \sqrt{\pi}\Lambda\kappa^2\right)\exp\left(-\sqrt{\pi}\Lambda\kappa\right). \tag{14}$$

Although we only study the 2D Yukawa systems here, Eq. (13) is generally correct for all R systems in principle with different interaction potentials, which can be fitted by the eIPL potential [10,69]. Note that, to characterize our studied 2D Yukawa systems, we always use the screening parameter κ, rather than the number density n or Wigner-Seitz radius a; as a result, we rewrite $h(n)$ as the function of κ, as described above.

As the first major result of this paper, we obtain the analytical isomorphic curves for 2D Yukawa systems by substituting the $h(\kappa)$'s expression of Eq. (14) into Eq. (6). Since the coupling parameter $\Gamma = Q^2/4\pi\epsilon_0 a k_B T$, the analytical isomorphic curves for 2D Yukawa systems can be further simplified to

$$\Gamma = \frac{\mathcal{C}\Lambda\ \exp\left(\sqrt{\pi}\Lambda\kappa\right)}{1 + \sqrt{\pi}\Lambda\kappa + (\sqrt{\pi}\Lambda\kappa)^2/2}, \tag{15}$$

where $\mathcal{C} = Q^2\mathcal{K}/8\epsilon_0\sqrt{\pi}\mathcal{A}$ is an arbitrary constant. Moreover, based on the expression of $h(\kappa)$, we are able to derive the analytical expression of the density-scaling exponent γ from Eq. (7), which is just

$$\gamma = \frac{1}{2} + \frac{(\sqrt{\pi}\Lambda\kappa)^3/4}{1 + \sqrt{\pi}\Lambda\kappa + (\sqrt{\pi}\Lambda\kappa)^2/2}. \tag{16}$$

We are able to obtain the specific expression for γ along an isomorphic curve from either one determined γ value from simulation or the Λ value from a determined isomorphic curve of Eq. (15). In Fig. 2, the dashed curve corresponds to the analytical density-scaling exponent of Eq. (16) with determined $\Lambda \approx 0.957$ for $\Gamma/\Gamma_m = 1.0$, well overlapping with the data points of $\Gamma/\Gamma_m = 1.0$. For $\Gamma/\Gamma_m = 1.0$, the relative difference of γ between Eq. (16) and the data points from our simulations in Fig. 2 is less than 5.2%, further confirming the accuracy of Eq. (16). Note that, from the isomorph theory [5], the γ value is only dependent on the number density n; however, our simulation results indicate that the γ value is also related to the temperature. We believe the temperature-related γ value is reasonable because the isomorph theory is only an approximation, so that the Λ value varies slightly under different conditions as we discuss in Sec. III C.

C. Melting curve prediction

From the previous investigations [4,5,13,60,65,72], the melting curve is predicted to be an isomorphic curve for R systems. We are able to confirm this conclusion through the definition of the isomorphic state [5]. If two state points $\mathbf{R}_1 \in (n_1, T_1)$ and $\mathbf{R}_2 \in (n_2, T_2)$ are isomorphic, then they should have the same reduced collective position vector $n_1^{-1/2}\mathbf{R}_1 = n_2^{-1/2}\mathbf{R}_2$ and the proportional configuration Boltzmann factors $\exp[-U(\mathbf{R}_1)/k_B T_1] \cong C_{12}\exp[-U(\mathbf{R}_2)/k_B T_2]$ [5]. Obviously, the configuration Boltzmann factors of solids are definitely different from those for liquids, so that the isomorphic curves cannot cross the melting curve, i.e., the melting curve is an isomorphic curve [64].

In fact, we find that the previously obtained melting curves of 2D Yukawa systems also exhibit the isomorphic properties. From the previous investigations of 2D Yukawa systems relying on computer simulations under vast ranges of conditions [56,57], 2D Yukawa liquids with the same effective coupling parameter Γ^* exhibit the same properties using different structural measures [55–57], clearly indicating the approximately invariant structure. Furthermore, in Ref. [55], the melting curve of 2D Yukawa systems derived from Lindemann's melting criterion [58] just corresponds to the approximately invariant dynamics. In fact, by directly substituting the reduced nearest-neighbor distance of $\Lambda = 1$ into the isomorphic curves of Eq. (15) above, we just obtain Eq. (1) of Ref. [55], further indicating that the melting curve for 2D Yukawa systems is an isomorphic curve. Additionally, as investigated in Ref. [60], the dynamics of 2D Yukawa liquids exhibit the isomorph invariant of the reduced transverse sound speed, indicating that the supercritical transition between the liquidlike and gaslike states is also an isomorphic curve.

To derive the melting curve of 2D Yukawa systems using the isomorphic curves of Eq. (15), we only need to determine the two unknown quantities of Λ and $\mathcal{C}$ there. A

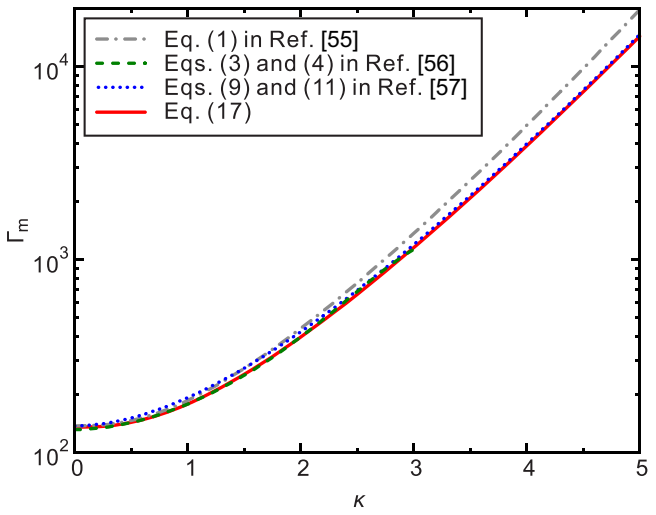

FIG. 4. Our derived analytical melting curve from the isomorph theory for 2D Yukawa systems, as well as the melting curves from the previous investigations of Refs. [55–57]. Clearly, our obtained melting curve overlaps well with the previously obtained melting curves in Refs. [55–57], indicating their agreement. Different from Refs. [55–57], our derived melting curve comes from the isomorphic curves of Eq. (15), combined with two known melting points of $\Gamma_m \approx 177.9$ and 395.5 for $\kappa = 1.0$ and 2.0, respectively, which can be further extended to the range of $\kappa > 5.0$. Note that the values of the effective coupling parameter Γ^* in the previously obtained melting curves are 137, 131, and 137 in Refs. [55–57], respectively.

reasonable approach of determining these two unknown quantities is just relying on at least two accurate melting points from the previous investigations directly. Here, we just choose two melting points of 2D Yukawa systems from Ref. [56], which are $\Gamma_m \approx 177.9$ for $\kappa = 1.0$ and $\Gamma_m \approx 395.5$ for $\kappa = 2.0$, respectively. Substituting these two melting points into Eq. (15), we determine the values of these two unknown quantities, i.e., $\mathcal{C} \approx 140.936$ and $\Lambda \approx 0.957$. Again, substituting these determined values of $\mathcal{C}$ and Λ into Eq. (15), we directly derive the melting curve from the isomorphic property as

$$\Gamma_m = \frac{134.902\ \exp(1.697\kappa)}{1 + 1.697\kappa + (1.697\kappa)^2/2}. \tag{17}$$

Our obtained melting curve of Eq. (17) for 2D Yukawa systems is just the second major result of this paper. Note that, while choosing two different melting points under different κ values in the equation derivation, the obtained expression of the melting curve may be different from Eq. (17). However, while plotting these derived melting curves with different expressions, we find that they are very close and even overlap together.

In Fig. 4, we present our derived analytical melting curve of 2D Yukawa systems, i.e., Eq. (17), with the previously obtained three melting curves in Refs. [55–57], which have already been widely accepted and validated. Clearly, our derived melting curve almost completely overlaps with the previous three melting curves in Refs. [55–57] combined with $\Gamma^* = 137$, 131, and 137, respectively, further indicating the accuracy of our derived Eq. (17). One advantage of our melting curve of Eq. (17) is that this expression can be further extended to the range of $\kappa > 5.0$ to predict the melting points there. Note that the slight uncertainties of the coefficients Λ and $\mathcal{C}$ in Eq. (15) may come from the inaccuracy of the two chosen melting points, which would lead to an exaggerated error while extending Eq. (17) into the range far away from $\kappa \leqslant 5.0$.

Actually, the concept of the effective coupling parameter Γ^* raised in the previous investigations [73–76] is similar to the isomorphic properties studied here. In Refs. [55–57,74–76], it is demonstrated that 2D Yukawa systems with the same effective coupling parameter Γ^* exhibit nearly the same radial distribution function $g(r)$, just corresponding to the invariant structure, no matter how κ varies. The concept of Γ^* is proposed to use only one single parameter Γ^* to determine a series of similar Yukawa systems analogous to the coupling parameter of the one-component plasma system [57], i.e., Γ^* is the combination of both Γ and κ. For $\Gamma^* \gtrsim 40$, $\Gamma^*(\Gamma, \kappa)$ is able to be approximately expressed using the variable separation [56,57], i.e., the ratio of Γ/Γ^* is the function of only one variable κ. However, for smaller Γ^* values, $\Gamma^*(\Gamma, \kappa)$ cannot be expressed using variable separation anymore, i.e., the ratio Γ/Γ^* depends on both Γ^* and κ as shown in Fig. 2(b) of Ref. [56] and Fig. 7 of Ref. [57].

From our derivation of the isomorphic curves above, we are able to explain this interesting feature of $\Gamma^* \lesssim 40$ found in [56,57]. The effective coupling parameter Γ^* in Refs. [55–57] can be expressed as $\Gamma^* = \mathcal{C}\Lambda$ in our derivation of the isomorphic curves, because Γ^* is tailored to converge to Γ as κ goes to zero [57]. Therefore, we obtain $\Gamma/\Gamma^* = \exp(\sqrt{\pi}\Lambda\kappa)/[1 + \sqrt{\pi}\Lambda\kappa + (\sqrt{\pi}\Lambda\kappa)^2/2]$, which depends on both the reduced nearest-neighbor distance Λ and the κ value. For lower Γ^* values, the location of the first peak of $g(r)$ is a little bit closer to the zero point, so that the corresponding Λ value diminishes slightly. However, for higher Γ^* values, the variation of the location of the first peak of $g(r)$ is negligible. As a result, the slightly varying Λ value for $\Gamma^* \lesssim 40$ results in the complicated expression of Γ^* that cannot be expressed using the variable separation, as found in Refs. [56,57]. In fact, instead of a constant, Λ is a variable related to s_{ex} from the generalized isomorphic curves $h(n, s_{ex})/k_BT = \text{const}$ [69], obtained from the isomorph invariant of $g(r)$, not the isomorph theory.

IV. SUMMARY

In summary, we derive the analytical isomorphic curves and melting curve of 2D Yukawa systems from the isomorph theory. To confirm that our derivation is reliable, we perform molecular dynamical simulations under various conditions to demonstrate that the isomorph theory does work for 2D Yukawa systems. After verifying that the Yukawa potential is well fitted by the eIPL potential around the first peak of $g(r)$, we use the local effective power-law exponent of the Yukawa potential to obtain the analytical isomorphic curves, as well as the analytical density-scaling exponent of 2D Yukawa systems. We find that the melting curve of 2D Yukawa systems

can be well predicted from our obtained isomorphic curves of Eq. (15) combined with two known melting points. Our obtained melting curve of Eq. (17) well agrees with the previous melting results for 2D Yukawa systems using completely different approaches [55–57]. Based on the isomorphic curves of Eq. (15), we also provide our interpretation for the dependence of the effective coupling parameter Γ^* on the nearest-neighbor distance.

ACKNOWLEDGMENTS

This work was supported by the National Natural Science Foundation of China under Grants No. 12175159, No. 12305220, and No. 12247163, the Excellent Postdoctoral Program of Jiangsu Province, the 1000 Youth Talents Plan, startup funds from Soochow University, and the Priority Academic Program Development of Jiangsu Higher Education Institutions.

[1] N. P. Bailey, U. R. Pedersen, N. Gnan, T. B. Schrøder, and J. C. Dyre, J. Chem. Phys. **129**, 184507 (2008).
[2] N. P. Bailey, U. R. Pedersen, N. Gnan, T. B. Schrøder, and J. C. Dyre, J. Chem. Phys. **129**, 184508 (2008).
[3] T. B. Schrøder, N. P. Bailey, U. R. Pedersen, N. Gnan, and J. C. Dyre, J. Chem. Phys. **131**, 234503 (2009).
[4] T. B. Schrøder, N. Gnan, U. R. Pedersen, N. P. Bailey, and J. C. Dyre, J. Chem. Phys. **134**, 164505 (2011).
[5] N. Gnan, T. B. Schrøder, U. R. Pedersen, N. P. Bailey, and J. C. Dyre, J. Chem. Phys. **131**, 234504 (2009).
[6] J. C. Dyre, J. Phys. Chem. B **118**, 10007 (2014).
[7] U. R. Pedersen, N. P. Bailey, T. B. Schrøder, and J. C. Dyre, Phys. Rev. Lett. **100**, 015701 (2008).
[8] T. S. Ingebrigtsen, T. B. Schrøder, and J. C. Dyre, Phys. Rev. X **2**, 011011 (2012).
[9] T. S. Ingebrigtsen, L. Bøhling, T. B. Schrøder, and J. C. Dyre, J. Chem. Phys. **136**, 061102 (2012).
[10] A. K. Bacher, T. B. Schrøder, and J. C. Dyre, Nat. Commun. **5**, 5424 (2014).
[11] N. P. Bailey, L. Bøhling, A. A. Veldhorst, T. B. Schrøder, and J. C. Dyre, J. Chem. Phys. **139**, 184506 (2013).
[12] T. B. Schrøder and J. C. Dyre, J. Chem. Phys. **141**, 204502 (2014).
[13] U. R. Pedersen, L. Costigliola, N. P. Bailey, T. B. Schrøder, and J. C. Dyre, Nat. Commun. **7**, 12386 (2016).
[14] H. M. Thomas and G. E. Morfill, Nature (London) **379**, 806 (1996).
[15] L. I, W.-T. Juan, C. H. Chiang, and J. H. Chu, Science **272**, 1626 (1996).
[16] A. Melzer, A. Homann, and A. Piel, Phys. Rev. E **53**, 2757 (1996).
[17] R. L. Merlino and J. A. Goree, Phys. Today **57**, 32 (2004).
[18] V. E. Fortov, A. V. Ivlev, S. A. Khrapak, A. G. Khrapak, and G. E. Morfill, Phys. Rep. **421**, 1 (2005).
[19] G. E. Morfill and A. V. Ivlev, Rev. Mod. Phys. **81**, 1353 (2009).
[20] M. Bonitz, C. Henning, and D. Block, Rep. Prog. Phys. **73**, 066501 (2010).
[21] A. Piel, *Plasma Physics* (Springer, Heidelberg, 2010).
[22] U. Konopka, G. E. Morfill, and L. Ratke, Phys. Rev. Lett. **84**, 891 (2000).
[23] G. J. Kalman, P. Hartmann, Z. Donkó, and M. Rosenberg, Phys. Rev. Lett. **92**, 065001 (2004).
[24] S. Nunomura, J. Goree, S. Hu, X. Wang, A. Bhattacharjee, and K. Avinash, Phys. Rev. Lett. **89**, 035001 (2002).
[25] V. Nosenko, S. Zhdanov, A. V. Ivlev, G. Morfill, J. Goree, and A. Piel, Phys. Rev. Lett. **100**, 025003 (2008).
[26] P. Hartmann, A. Douglass, J. C. Reyes, L. S. Matthews, T. W. Hyde, A. Kovács, and Z. Donkó, Phys. Rev. Lett. **105**, 115004 (2010).
[27] L. Couëdel, V. Nosenko, A. V. Ivlev, S. K. Zhdanov, H. M. Thomas, and G. E. Morfill, Phys. Rev. Lett. **104**, 195001 (2010).
[28] H. Kählert, J. Carstensen, M. Bonitz, H. Löwen, F. Greiner, and A. Piel, Phys. Rev. Lett. **109**, 155003 (2012).
[29] P. Hartmann, A. Z. Kovács, A. M. Douglass, J. C. Reyes, L. S. Matthews, and T. W. Hyde, Phys. Rev. Lett. **113**, 025002 (2014).
[30] G. Gogia and J. C. Burton, Phys. Rev. Lett. **119**, 178004 (2017).
[31] V. Nosenko and J. Goree, Phys. Rev. Lett. **93**, 155004 (2004).
[32] P. Hartmann, J. C. Reyes, E. G. Kostadinova, L. S. Matthews, T. W. Hyde, R. U. Masheyeva, K. N. Dzhumagulova, T. S. Ramazanov, T. Ott, H. Kählert, M. Bonitz, I. Korolov, and Z. Donkó, Phys. Rev. E **99**, 013203 (2019).
[33] C. R. Du, V. Nosenko, H. M. Thomas, Y. F. Lin, G. E. Morfill, and A. V. Ivlev, Phys. Rev. Lett. **123**, 185002 (2019).
[34] M. Zuzic, A. V. Ivlev, J. Goree, G. E. Morfill, H. M. Thomas, H. Rothermel, U. Konopka, R. Sütterlin, and D. D. Goldbeck, Phys. Rev. Lett. **85**, 4064 (2000).
[35] J. Pramanik, G. Prasad, A. Sen, and P. K. Kaw, Phys. Rev. Lett. **88**, 175001 (2002).
[36] O. Arp, D. Block, A. Piel, and A. Melzer, Phys. Rev. Lett. **93**, 165004 (2004).
[37] E. Thomas, Jr. and J. Williams, Phys. Rev. Lett. **95**, 055001 (2005).
[38] G. E. Morfill, H. M. Thomas, U. Konopka, H. Rothermel, M. Zuzic, A. Ivlev, and J. Goree, Phys. Rev. Lett. **83**, 1598 (1999).
[39] M. Bonitz, D. Block, O. Arp, V. Golubnychiy, H. Baumgartner, P. Ludwig, A. Piel, and A. Filinov, Phys. Rev. Lett. **96**, 075001 (2006).
[40] Y.-Y. Tsai, J.-Y. Ysai, and L. I, Nat. Phys. **12**, 573 (2016).
[41] M. S. Murillo, Phys. Rev. Lett. **85**, 2514 (2000).
[42] V. Nosenko, J. Goree, and A. Piel, Phys. Rev. Lett. **97**, 115001 (2006).
[43] M. Schwabe, K. Jiang, S. Zhdanov, T. Hagl, P. Huber, A. V. Ivlev, A. M. Lipaev, V. I. Molotkov, V. N. Naumkin, K. R. Sütterlin, H. M. Thomas, V. E. Fortov, G. E. Morfill, A. Skvortsov, and S. Volkov, Europhys. Lett. **96**, 55001 (2011).
[44] H. Ohta and S. Hamaguchi, Phys. Plasmas **7**, 4506 (2000).
[45] J. Ashwin and A. Sen, Phys. Rev. Lett. **114**, 055002 (2015).
[46] S. Singh, P. Bandyopadhyay, K. Kumar, and A. Sen, Phys. Rev. Lett. **129**, 115003 (2022).
[47] Y. F. He, B. Q. Ai, C. X. Dai, C. Song, R. Q. Wang, W. T. Sun, F. C. Liu, and Y. Feng, Phys. Rev. Lett. **124**, 075001 (2020).
[48] S. Hamaguchi, R. T. Farouki, and D. H. E. Dubin, Phys. Rev. E **56**, 4671 (1997).

[49] S. A. Khrapak, B. A. Klumov, P. Huber, V. I. Molotkov, A. M. Lipaev, V. N. Naumkin, H. M. Thomas, A. V. Ivlev, G. E. Morfill, O. F. Petrov, V. E. Fortov, Yu. Malentschenko, and S. Volkov, Phys. Rev. Lett. **106**, 205001 (2011).
[50] S. A. Khrapak, B. A. Klumov, P. Huber, V. I. Molotkov, A. M. Lipaev, V. N. Naumkin, A. V. Ivlev, H. M. Thomas, M. Schwabe, G. E. Morfill, O. F. Petrov, V. E. Fortov, Yu. Malentschenko, and S. Volkov, Phys. Rev. E **85**, 066407 (2012).
[51] S. A. Khrapak, Phys. Rev. Res. **2**, 012040(R) (2020).
[52] A. Melzer, *Physics of Dusty Plasmas* (Springer Nature, Switzerland AG, 2019).
[53] D. Huang, S. Lu, M. S. Murillo, and Y. Feng, Phys. Rev. Res. **4**, 033064 (2022).
[54] X. Wang, A. Bhattacharjee, and S. Hu, Phys. Rev. Lett. **86**, 2569 (2001).
[55] O. S. Vaulina and I. E. Dranzhevski, Phys. Scr. **73**, 577 (2006).
[56] P. Hartmann, G. J. Kalman, Z. Donkó, and K. Kutasi, Phys. Rev. E **72**, 026409 (2005).
[57] T. Ott, M. Stanley, and M. Bonitz, Phys. Plasmas **18**, 063701 (2011).
[58] F. A. Lindemann, Phys. Z. **11**, 609 (1910).
[59] F. Melandsø, Phys. Plasmas **3**, 3890 (1996).
[60] N. Yu, D. Huang, S. Lu, S. Khrapak, and Y. Feng, Phys. Rev. E **109**, 035202 (2024).
[61] D. Huang, M. Baggioli, S. Lu, Z. Ma, and Y. Feng, Phys. Rev. Res. **5**, 013149 (2023).
[62] Y. Rosenfeld, Phys. Rev. A **15**, 2545 (1977).
[63] Y. Rosenfeld, J. Phys.: Condens. Matter **11**, 5415 (1999).
[64] A. A. Veldhorst, T. B. Schrøder, and J. C. Dyre, Phys. Plasmas **22**, 073705 (2015).
[65] J. C. Dyre, Phys. Rev. E **88**, 042139 (2013).
[66] T. H. Berlin and E. W. Montroll, J. Chem. Phys. **20**, 75 (1952).
[67] A. A. Veldhorst, J. C. Dyre, and T. B. Schrøder, J. Chem. Phys. **141**, 054904 (2014).
[68] F. L. Castello, P. Tolias, J. S. Hansen, and J. C. Dyre, Phys. Plasmas **26**, 053705 (2019).
[69] L. Bøhling, N. P. Bailey, T. B. Schrøder, and J. C. Dyre, J. Chem. Phys. **140**, 124510 (2014).
[70] C. Liang, D. Huang, S. Lu, and Y. Feng, Phys. Rev. Res. **5**, 033086 (2023).
[71] S. Lu, D. Huang, C. Liang, and Y. Feng, Phys. Rev. Res. **5**, 043116 (2023).
[72] L. Friedeheim, F. Hummel, J. C. Dyre, and N. P. Bailey, Phys. Rev. B **109**, 104109 (2024).
[73] O. S. Vaulina and S. A. Khrapak, J. Exp. Theor. Phys. **90**, 287 (2000).
[74] O. Vaulina, S. Khrapak, and G. Morfill, Phys. Rev. E **66**, 016404 (2002).
[75] O. S. Vaulina and S. V. Vladimirov, Phys. Plasmas **9**, 835 (2002).
[76] V. E. Fortov, O. S. Vaulina, O. F. Petrov, V. I. Molotkov, A. M. Lipaev, V. M. Torchinsky, H. M. Thomas, G. E. Morfill, S. A. Khrapak, Yu. P. Semenov, A. I. Ivanov, S. K. Krikalev, A. Yu. Kalery, S. V. Zaletin, and Yu. P. Gidzenko, Phys. Rev. Lett. **90**, 245005 (2003).